Original Article: Open Access

VIBGYOR online

International Journal of
Metallurgy and Metal Physics

Microstructure and Electrochemical Behaviour of TiB_2 Reinforced Titanium Matrix Composites Fabricated by Spark Plasma Sintering in Simulated Body Fluid Environment

Maseko SW[1*], Popoola API[1], Kgoete F[1] and Fayomi OSI[1,2]

[1]*Department of Chemical, Metallurgical, and Materials Engineering, Tshwane University of Technology, South Africa*

[2]*Department of Mechanical Engineering, Covenant University, Nigeria*

Abstract

Titanium and its alloys are one of the most highly used metallic materials in modern materials engineering; its use range from aerospace, defence, and biomedical applications. However, this material has relatively poor corrosion resistance in biomedical applications; this is due to aggressive anodic ions present in physiological fluids. In this study, powder metallurgical processes were employed to enhance the properties of titanium through the dispersion of TiB_2 ceramic particulates into the matrix. The consolidation of the admixed powders was carried out using spark plasma sintering (SPS). The microstructure and phase analysis of the sintered composites was carried out using optical microscope (OM), scanning electron microscope (SEM) and X-ray diffractometer (XRD), while the hardness was determined using Vickers' microhardness tester. The electrochemical characteristics of the composites were carried out using potentiostat with the three-electrode method. The OM, SEM and XRD results confirmed the enhancement of the matrix properties through dispersion strengthening and grain refinement. The corrosion resistance was observed to have a direct relationship with the composition of the reinforcement materials.

Keywords

SPS, Corrosion, Matrix, Reinforcement, TiB whiskers

Introduction

The development of advanced materials that out-perform existing materials is an area which is in the fore front of materials engineering. Materials such as titanium are one of the most important and widely used engineering materials; due to its use in a wide variety of heavy and light engineering applications. This metal has found extensive use in biomedical applications; this is driven by its attractive properties such as excellent biocompatibility, high strength to weight ratio, low density, and good corrosion resistance [1]. However, the physiological human fluids are composed of aggressive anion species and dissolved gases which may cause accelerated dissolution of the titanium passive oxide layer. Corrosion attack of implants has adverse effects on the titanium's biocompatibility and mechanical integrity [2,3]. Various methods have been undertaken to enhance the performance of titanium-based biomaterials, the use of ceramic phases has been studied as one of the most viable options to enhance the anti-corrosion performance of titanium-based biomaterials. The use of boron-based materials for the improvement of anti-corrosion properties of titanium-based materials has been widely researched. However, most studies in open literature investigated the use of boron-based materials as a coating material using different surface modification techniques

***Corresponding author:** *Maseko SW, Department of Chemical, Metallurgical, and Materials Engineering, Tshwane University of Technology, Pretoria, South Africa*

Accepted: August 13, 2018: **Published:** August 15, 2018

Citation: Maseko SW, Popoola API, Kgoete F, Fayomi OSI (2018) Microstructure and Electrochemical Behaviour of TiB_2 Reinforced Titanium Matrix Composites Fabricated by Spark Plasma Sintering in Simulated Body Fluid Environment. Int J Metall Met Phys 3:018

[4,5]. Titanium reacts with the boron phase to forms need-like TiB whiskers which form on the interface and thus enhance the corrosion performance of the matrix. Most studies have been conducted inducing TiB whiskers through surface-based methods such as plasma paste boriding and other boriding techniques [4,6-8]. However, the use of surface modification technologies is limited by its dependence on coating adhesion strength between the surface of the titanium substrate and TiB coating. Therefore, there is a need of the development of titanium-based materials fabricated by bulk modification techniques through the incorporation of boron-based reinforcements. Powder metallurgy (PM) remains one of the most advantageous processing techniques in bulk materials engineering. Spark plasma sintering (SPS) is one of the emerging sintering technologies used to consolidate a wide variety of powder materials. It is a unique sintering technology that utilizes direct current (DC) as a heating mechanism, and high applied pressure to fabricate compacts with minimal degree of porosity [9]. The processing of Ti matrix using TiB_2 using SPS has been investigated by [10], the authors investigated the spark plasma sintering of Ti-TiB_2 composites. However, the study did not entail the investigation of electrochemical behaviour of the composites. This study aims to fabricate a titanium-based composite with enhanced electrochemical behaviour through the incorporation of ceramic particulates.

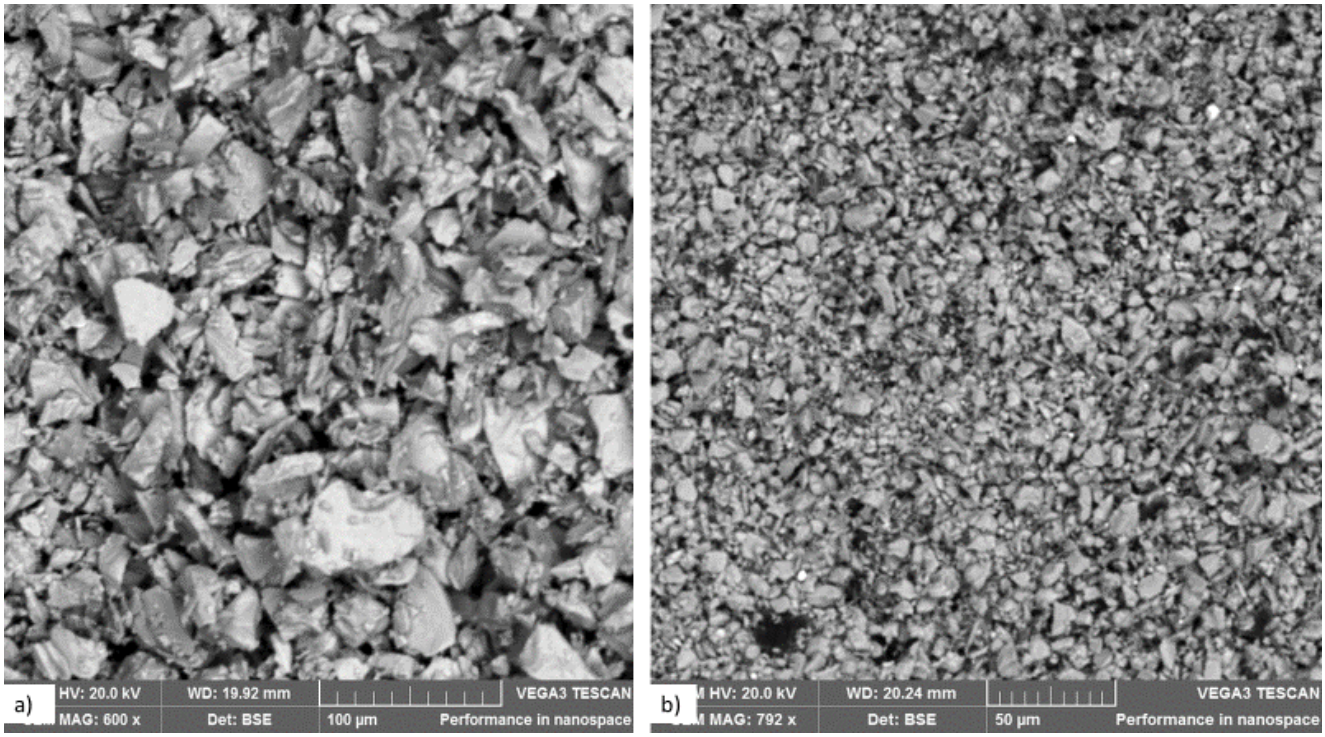

Figure 1: SEM micrographs of feedstock powders: a) CpTi and b) TiB_2 powders.

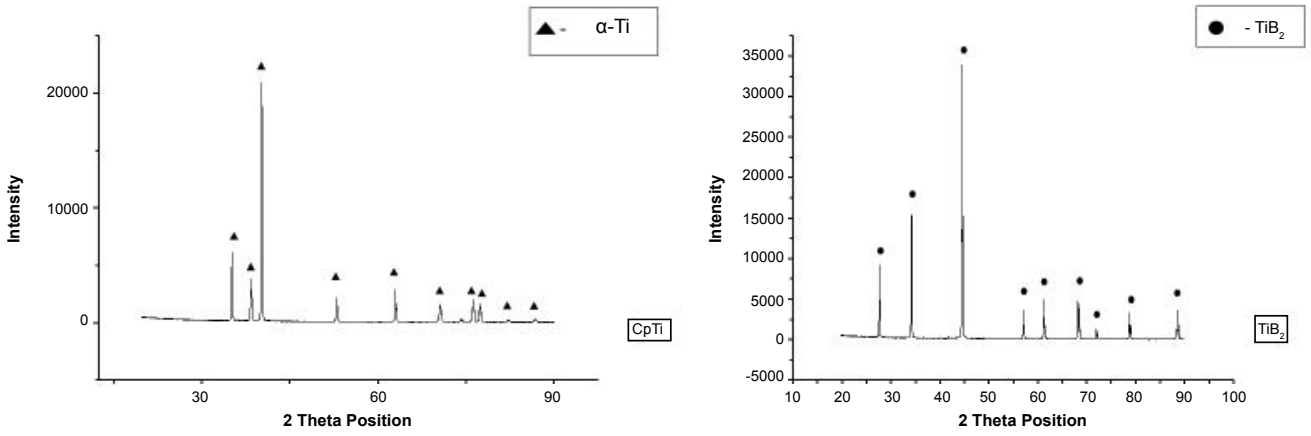

Figure 2: XRD spectra of the feedstock powders: a) CpTi and b) TiB_2 powders.

Citation: Maseko SW, Popoola API, Kgoete F, Fayomi OSI (2018) Microstructure and Electrochemical Behaviour of TiB_2 Reinforced Titanium Matrix Composites Fabricated by Spark Plasma Sintering in Simulated Body Fluid Environment. Int J Metall Met Phys 3:018

Experimental

Feedstock materials

In this study, fine commercially pure titanium (CpTi) powder supplied by Merck Millipore (with less than 150 μm particle size, 98% purity) was used as the matrix material. TiB_2 powder supplied by Merck Millipore was used as the reinforcement material (with less than 90 μm particle size, 99.9% purity. Figure 1 contains SEM images containing particle morphology of CpTi and TiB_2 feedstock powders. This figure shows an irregular-shaped morphology for both powders. Figure 2 is the XRD spectra of CpTi and TiB_2 raw powders. This figure shows that the powders are of high purity and no contaminants were detected during scanning.

Powder mixing

The powder materials were mixed using the PM 400 high energy ball mill at 300 rpm for 8 hours with 3 agate balls to enhance the mixing kinetics. Three composites were prepared, with reinforcement composition of 5, 10, 15 wt% TiB_2 (Table 1).

Table 1: Sample ID and composition of Ti-TiB_2 binary composites.

Composition	Sample ID
95Ti-5 wt% TiB_2	Sample 1
80Ti-10 wt% TiB_2	Sample 2
85Ti-15 wt% TiB_2	Sample 3

Powder consolidation

The mixed samples were then densified using the SPS furnace (HPD5, FCT Systeme GmbH). The admixed powders were densified at a temperature of 1300 °C, at an applied load of 50 MPa, 5 min dwell time, and heating rate of 100 °C/min under a vacuum atmosphere. The bulk density of the samples was determined prior to characterization to determine the degree of porosity in the resultant composites. The surface of samples was mechanically ground and polished using conventional metallographic procedures. The samples were then etched using Kroll's reagent to reveal the microstructure for downstream analysis.

Characterization of sintered composites

The microstructure and phase evolution of the sintered samples were investigated using a future-tech corp optical microscope (OM) (FM-800), Joel field emission scanning electron microscope (SEM) (JSM-7600F), and

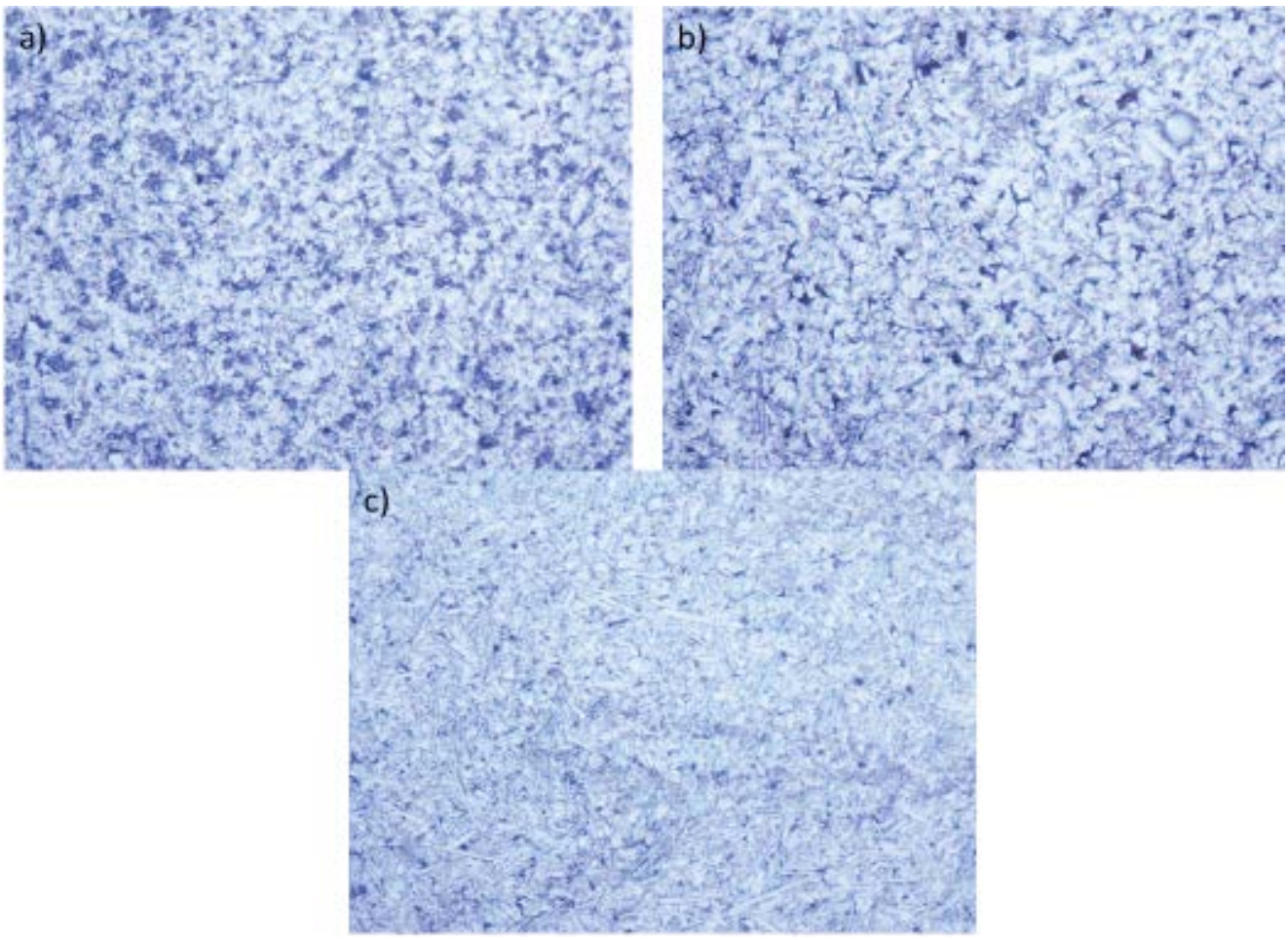

Figure 3: OM micrographs of Ti-TiB_2 binary composites: a) 95Ti-5 wt% TiB_2; b) 90Ti-10 wt% TiB_2, and c) 85Ti-15 wt% TiB_2.

PANalytical empyrean ray diffractometer (XRD). Back-scattered images (BSI) were collected from the prepared surfaces. Phase characterization was carried out at operating the XRD equipment at 30 kV and 30 mA, scan range of 0 to 90° at a scan rate of 5°/min, while Xpert highscore was used to analyse the spectra.

Electrochemical characterization

The anti-corrosion performance of the sintered samples was determined using linear polarization and open circuit potential (OCP) tests in simulated body fluid. A three-electrode system was used to determine the electrochemical behaviour of the composites. The composites were connected as the working electrode, with an $Ag/AgCl_2$ reference electrode, and a Pt counter electrode. The OCP was monitored for 3600 s to ensure stabilization. All electrochemical tests were conducted at room temperature. Tafel extrapolation was used to determine the corrosion characteristics of the composites.

Results and Discussion

Microstructure and phase characterization

Figure 3 shows OM micrographs of the sintered Ti-TiB_2 binary composites with varying compositions of TiB_2 reinforcement. Figure 3a depicts a microstructure with different structural make-up. The structures appear in bright and dark regions. The bright phases are flat and thin and match the description of α lamellar structures according to literature. The figure also shows little presence of TiB whiskers in its structure. Little to no evidence of β phase was observed in the micrographs. The figure also shows a significant dark phase of ceramic material which did not diffuse thoroughly during the application of heat and pressure during the SPS process. Figure 3b shows a decrease in the dark ceramic phase when compared to the Figure 3a. This figure also shows the definite emergence of the TiB needle-shaped whiskers dispersed homogenously throughout the matrix material. Figure 3c shows a more refined microstructure when compared to the previous two compositions; with a more distinguished formation of TiB whiskers dispersed throughout the matrix material. Grain refinement is an effective alternative route to material strengthening; this phenomenon is known to result in significant enhancement of the mechanical and physical properties of composites [11-13]. States that the presence of TiB needles in a titanium matrix is pronounced with significant increases in hardness of the composites. Therefore, significant improvements in hardness can be expected from the presence of TiB whiskers. SEM micrograph indicate two distinctive phases in its makeup (see Figure 4); its shows the dominant light grey phase which is titanium rich, and the black boride rich phases which dominantly in the form of TiB whiskers. Figure 5 is the XRD spectra of the Ti-TiB_2 binary composites. The XRD observations confirm the transformation of all the boron species (TiB_2) into TiB

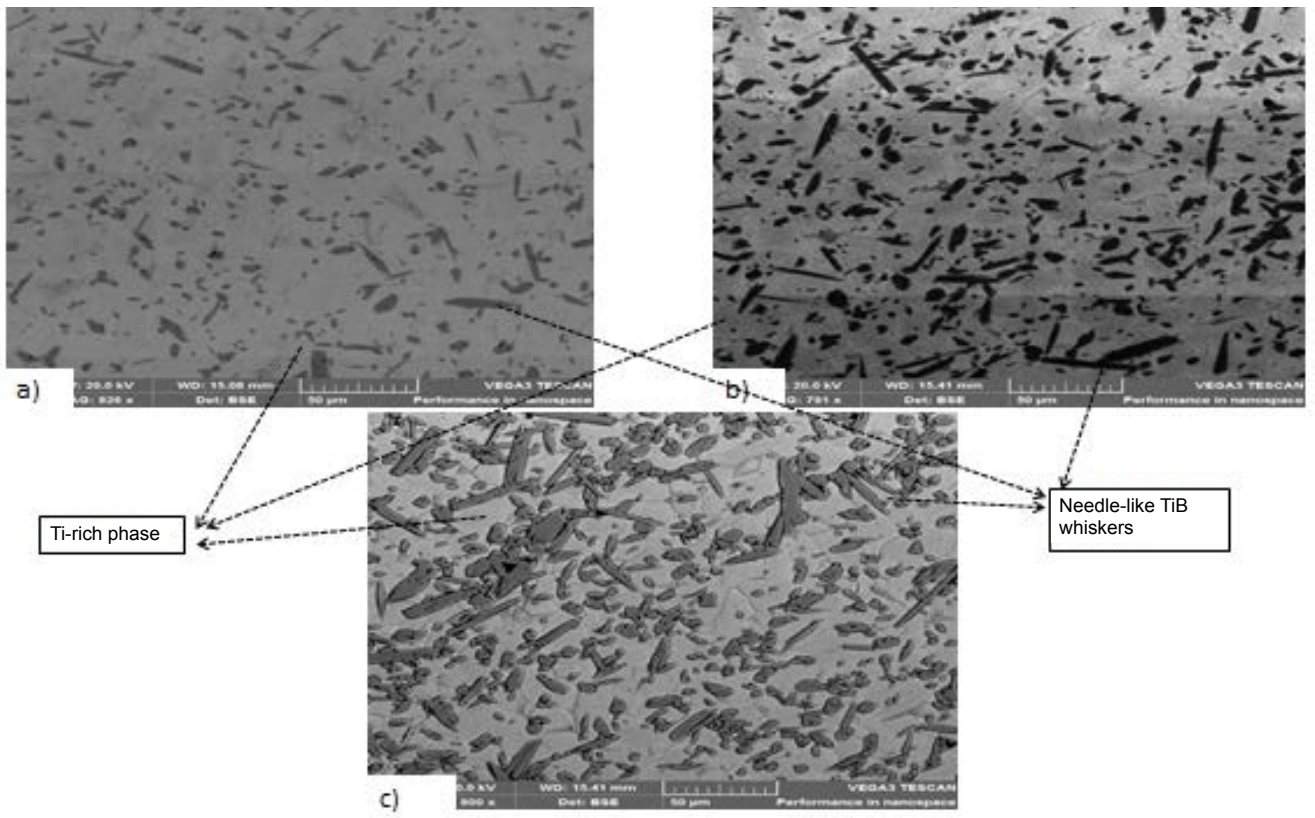

Figure 4: SEM Micrographs of Ti-TiB_2 binary composites: a) 95Ti-5 wt% TiB_2; b) 90Ti-10 wt% TiB_2; and c) 85Ti-15 wt% TiB_2.

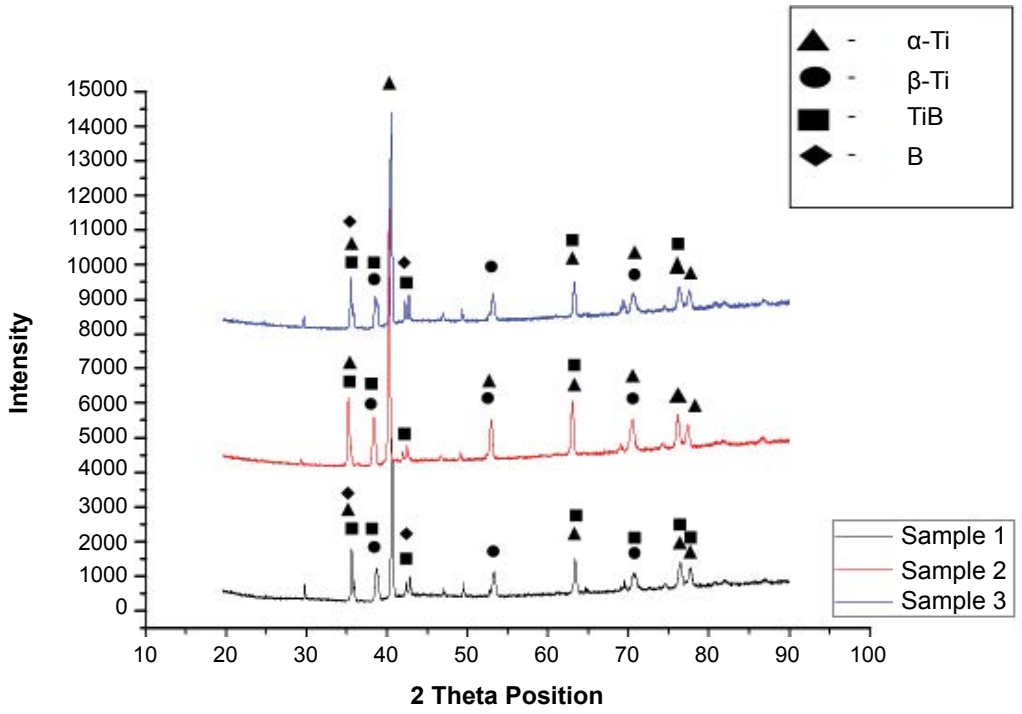

Figure 5: XRD patterns of Ti-TiB_2 binary composites.

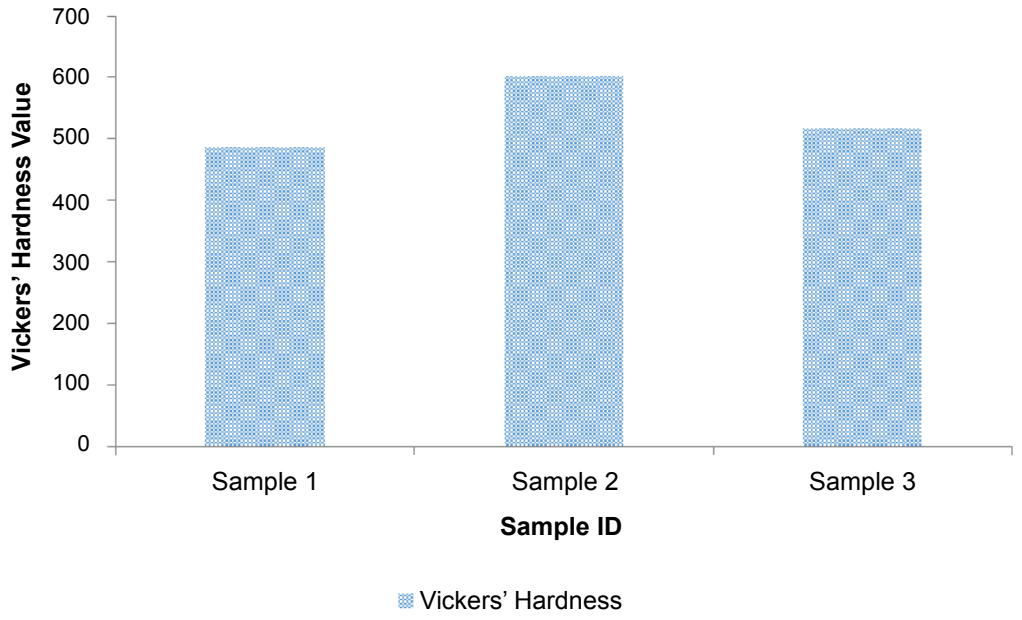

Figure 6: Hardness of Ti-TiB_2 binary composites.

in the resultant composite, with little quantities evolving to elemental boron. The patterns also showed that there is no presence of Ti_3B_4, which was a possible intermediate phase in the matrix. The results also depict the detection of the cubic β-Ti phase for all three composites: The β phase was detected at 2θ angles of approximately 37°, 55°, and 72° for all composites. The increase in reinforcement composition did not alter the occurrence of this phase, this suggests that the transformation of the α phase to β phase was mainly due to the thermo-mechanical characteristics associated with the SPS process.

Microhardness and relative density characterization

Figure 6 represents the hardness properties of the sintered Ti-TiB_2 binary composites. The hardness of the composites indicated significant increase for all composites. This is attributed to the dispersion strengthening effect achieved through the homogenous incorporation of hard ceramic

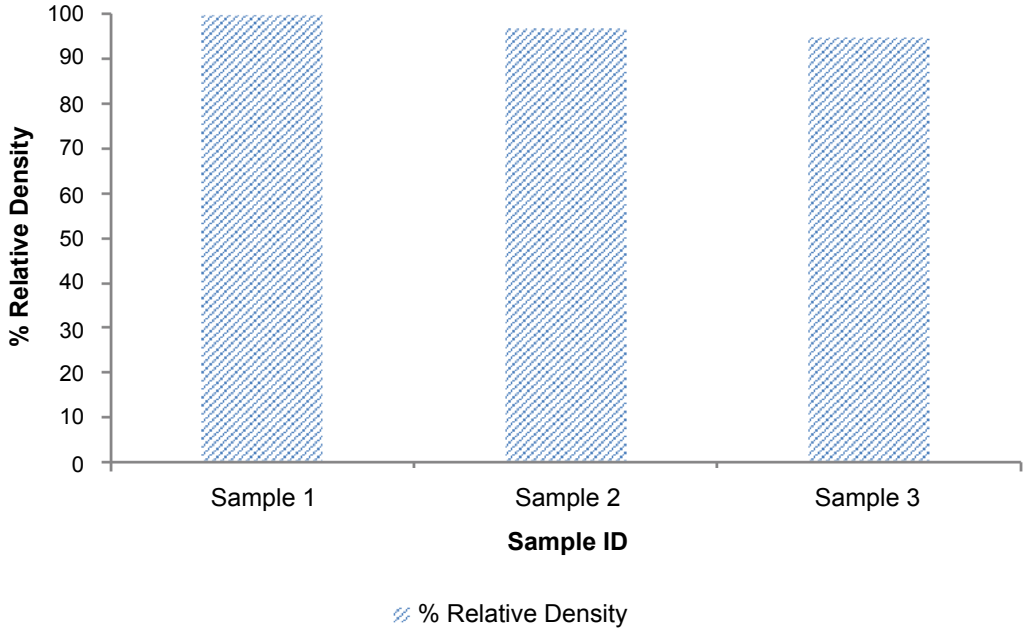

Figure 7: Percentage relative density of Ti-TiB_2 composites.

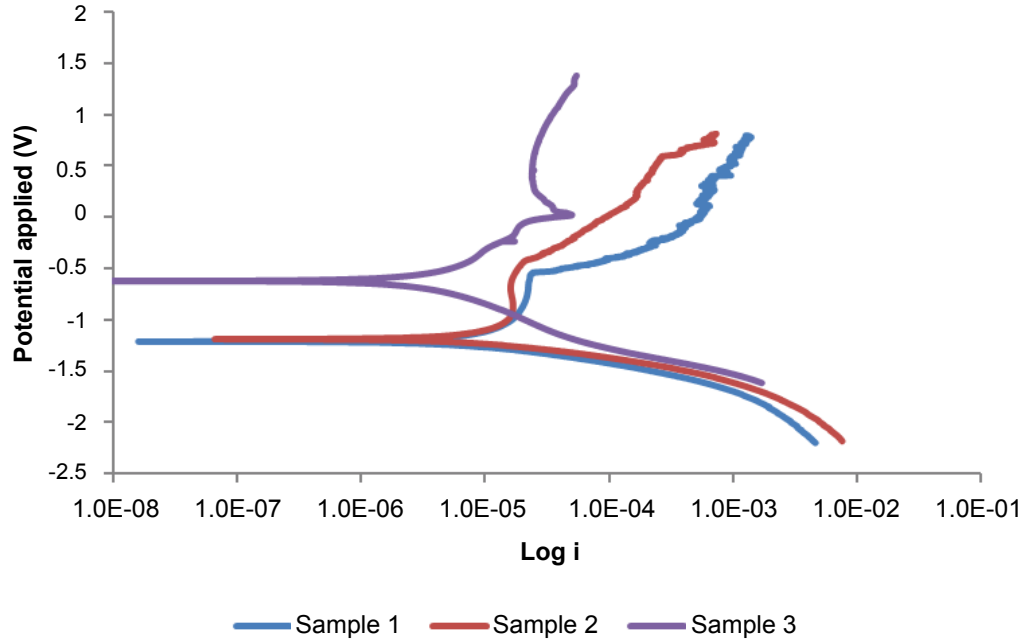

Figure 8: Linear polarization curves of Ti-TiB_2 composites.

particulates throughout the matrix. The composite with sample 2 (10 wt% TiB_2 reinforcement) showed the highest hardness compared to sample 1 and 3 (5 and 15 wt% TiB_2 composites). Although sample 3 has the highest reinforcement composition, its hardness was slightly lower than that of sample 2; which has a lower TiB_2 composition. This is due to the inherent increase in relative porosity in the bulk material as the reinforcement composition increases; this is attributed to the difference in thermal properties between the matrix and the reinforcement materials. The process parameters associated with SPS are known to have significant effects on the physical, mechanical, and chemical properties of the resultant composites [14]. Figure 7 represents the percentage relative density of the sintered specimens. Full densification was attained for sample 1, while sample 3 achieved the lowest bulk density. This indirect relationship between reinforcement composition and bulk density is attributed to the difference in thermal properties between the matrix and reinforcement materials.

Electrochemical characterization

The anti-corrosion performance of the binary com-

Table 2: Tafel Extrapolation Data of Ti-TiB_2 Composites.

Sample ID	Ecorr, Calc (V)	Ecorr, Obs (V)	jcorr (A/cm²)	icorr (A)	Corrosion rate (mm/year)	Polarization resistance (Ω)
Sample 1	-1.2093	-1.2136	1.21E-05	1.21E-05	0.041816	6798.8
Sample 2	-1.2156	-1.1901	1.27E-05	1.27E-05	0.041816	5921.9
Sample 3	-0.44425	-0.54626	6.54E-07	6.54E-07	0.022626	343020

posites is depicted by Figure 8 below. According to this figure, sample 3 has the best corrosion resistance when compared to sample 1 and 2. The curves show comparable electrochemical characteristics for sample 1 and 2, however, these composites showed little passivation characteristics when compared to sample 3 as there was a continuous steady change in current throughout the anodic region of the linear polarization curves. Table 2 shows the Tafel Extrapolation data of the composites. The corrosion resistance of the composites indicates a direct relationship with reinforcement composition. However, this contradicts findings observed in work carried by [3] regarding the effects of presence of pores on corrosion resistance. Sample 3 holds the best anti-corrosion performance, although it has the highest degree of porosity. This is attributed to the elimination of the bridging phenomenon by the SPS process. The presence of high quantities of TiB whiskers in this composite improved the corrosion resistance of the composite. Previous studies have indicated that the incorporation of ceramic particulates increase the corrosion resistance of the base metal; as the ceramic particles become an inert physical barrier to chemical attack [15,16].

Conclusion

SPS is a viable technique to fabricate materials with significantly enhanced properties at relatively lower sintering temperatures when compared to other conventional powder metallurgy processes. The methodology used in this study was effective in enhancing the properties of the titanium matrix material through dispersion strengthening and grain refinement strengthening as indicated by the micrographs of the composites. The electrochemical results show that porosity associated with an increase in reinforcement composition does not have a significant effect on the corrosion resistance of the composite materials; due to the role of the inert ceramic particulates.

Acknowledgement

This material is based upon work supported financially by the National Research Foundation. The authors also acknowledge the support from the Tshwane University of Technology, Pretoria, South Africa which helped to accomplish this work.

References

1. Lee Y, Niinomi M, Nakai M, Narita K, Cho K, et al. (2015) Wear transition of solid-solution-strengthened ti-29nb-13ta-4.6zr alloys by interstitial oxygen for biomedical applications. Journal of the Mechanical Behaviour of Biomedical Materials 51: 398-408.
2. Pocock G, Richards CD (2009) The human body: An introduction for the biomedical and health sciences. Oxford University Press.
3. Toptan F, Rego A, Alves AC, Guedes A (2016) Corrosion and tribocorrosion behaviour of ti-b4c composite intended for orthopaedic implants. Journal of The Mechanical Behaviour of Biomedical Materials 61: 152-163.
4. Sivakumar B, Singh R, Pathak LC (2015) Corrosion behavior of titanium boride composite coating fabricated on commercially pure titanium in Ringer's solution for bioimplant applications. Materials Science and Engineering: C 48: 243-255.
5. Makuch N, Kulka M, Keddam M, Taktak S, Ataibis V (2017) Growth kinetics and some mechanical properties of two-phase boride layers produced on commercially pure titanium during plasma paste boriding. Thin Solid Films 626: 25-37.
6. Çelikkan H, Öztürk MK, Aydin H, Aksu ML (2007) Boriding titanium alloys at lower temperatures using electrochemical methods. Thin Solid Films 515: 5348-5352.
7. Kaestner P, Olfe J, Rie KT (2001) Plasma-assisted boriding of pure titanium and TiAl6V4. Surface and Coatings Technology 142: 248-252.
8. Kartal G, Timur S, Urgen M, Erdemir A (2010) Electrochemical boriding of titanium for improved mechanical properties. Surface and Coatings Technology 204: 3935-3939.
9. Suarez M, Fernandez A, Menendez JL, Torrecillas R, Kessler HU, et al. (2013) Challenges and Opportunities for Spark Plasma Sintering: A key technology for a new generation of materials. In: Sintering Applications.
10. Erikson M, Salamon D, Nygren M, Shen Z (2008) Spark plasma sintering and deformation of Ti-TiB_2 Composites. Journal of Materials Science and Engineering A 475: 101-104.
11. Long Y, Zhang H, Wang T, Huang X, Li Y, et al. (2013) High-strength Ti-6Al-4V with ultrafine-grained structure fabricated by high energy ball milling and spark plasma sintering. Materials Science and Engineering: A 585: 408-414.
12. Yang C, Ni S, Liu Y, Song M (2015) Effects of sintering parameters on the hardness and microstructures of bulk bimodal titanium. Materials Science and Engineering: A 625: 264-270.
13. Selvakumar M, Chandradekar P, Mohanraj M, Ravisankar B, Balaraju JN (2015) Role of Powder Metallurgical Processing and TiB reinforcement on mechanical response of Ti-TiB composites. Materials Letters 144: 58-61.
14. Munir ZA, Anselmi-Tamburini U, Ohyanagi M (2006) The effect of electric field and pressure on the synthesis and consolidation of materials: A review of the spark plasma sintering method. Journal of Materials Science 41: 763-777.

15. Feng Q, Li T, Teng H, Zhang X, Zhang Y, et al. (2008) Investigation on the corrosion and oxidation resistance of Ni- Al_2O_3 nano-composite coatings prepared by sediment co- deposition. Surface and Coatings Technology 202: 4137-4144.

16. Seah KHW, Krishna M, Vijayalakshmi VT, Uchil J (2002) Corrosion behaviour of garnet particulate reinforced LM13 Al alloy MMCs. Corros Sci 44: 917-925.

Citation: Maseko SW, Popoola API, Kgoete F, Fayomi OSI (2018) Microstructure and Electrochemical Behaviour of TiB_2 Reinforced Titanium Matrix Composites Fabricated by Spark Plasma Sintering in Simulated Body Fluid Environment. Int J Metall Met Phys 3:018